

Analytic estimate of the maximum Lyapunov exponent in coupled-map lattices

F. Cecconi^{1,2,†}, and A. Politi^{3,2}

(1) *Dipartimento di Fisica, Università di Firenze*

(2) *INFN, Unità di Firenze*

(3) *Istituto Nazionale di Ottica, Firenze, Italy*

† *Also with INFN Sezione di Firenze*

()

Abstract

In this work we present a theoretical and numerical study of the behaviour of the maximum Lyapunov exponent for a generic coupled-map-lattice in the weak-coupling regime. We explain the observed results by introducing a suitable continuous-time formulation of the tangent dynamics. The first general result is that the deviation of the Lyapunov exponent from the uncoupled-limit limit is function of a single scaling parameter which, in the case of strictly positive multipliers, is the ratio of the coupling strength with the variance of local multipliers. Moreover, we find an approximate analytic expression for the Lyapunov exponent by mapping the problem onto the evolution of a chain of nonlinear Langevin equations, which are eventually reduced to a single stochastic equation. The probability distribution of this dynamical equation provides an excellent description for the behaviour of the Lyapunov exponent. Furthermore, multipliers with random signs are considered as well, finding that the Lyapunov exponent still depends on a single scaling parameter, which however has a different expression.

Short title: Maximum Lyapunov exponent in coupled-map lattices

05.45.-a

I. INTRODUCTION

Coupled-map lattices (CML) represent an interesting class of models for the investigation of several spatio-temporal phenomena, ranging from pattern formation to synchronization and to spatio-temporal chaos. Even though the discreteness of both space and time variables makes CML more amenable to numerical simulations than partial differential equations, the development of analytical techniques remains a difficult task. As usual, when dealing with hard problems, it is convenient to start from the identification of some relatively simple limit and thereby developing a perturbative approach. In the case of lattice dynamics, there are two opposite limits that are worth being investigated: the weak- and strong-coupling regime. In the former case, one can use all the knowledge acquired about low-dimensional systems to predict the dynamical properties when spatial directions are added. In this spirit, general theorems have been formulated and proved both about the structure of the invariant measure [1] and about the existence of travelling localized excitations [2]. The weak-coupling limit is interesting also in connections with the synchronization of chaotic attractors, a problem that can be effectively studied by looking at the behaviour of the Lyapunov exponents [3]. In the opposite limit, one expects a slow spatial dependence and, correspondingly, the existence of a few, dynamically active, degrees of freedom. This is the spirit that has led to studying different truncations of partial differential equations.

In this paper, we shall consider the most common indicator of chaos, the maximum Lyapunov exponent (MLE) in a lattice of coupled maps. It is known that a (weak) spatial coupling has a threefold consequence on the MLE: *i*) it naturally modifies the invariant measure; *ii*) it induces correlations among the local multipliers by coupling neighbouring sites; *iii*) it modifies the dynamics of perturbations by inducing a coupling in tangent space as well. The last phenomenon is the most interesting one, since it leads to counterintuitive effects like an increase of the MLE even in the presence of a stabilizing coupling.

In some previous papers [4,5], this problem has been addressed with a specific interest for the scaling behaviour of the MLE. However, the various approaches implemented so far have not been able to go beyond a qualitative explanation of the dependence on the coupling strength. Here, instead, we aim at presenting a fully quantitative, though approximate, treatment for the MLE in the small coupling regime. We restrict our analysis to the usual diffusive coupling scheme, but we are confident that the present approach can be effectively adapted to different (short-range) interaction schemes. More specifically, we refer to the dynamical equation

$$\begin{aligned} x_i(t+1) &= f(y_i(t+1)) \\ y_i(t+1) &= \varepsilon x_{i-1}(t) + (1-2\varepsilon)x_i(t) + \varepsilon x_{i+1}(t). \end{aligned} \quad (1)$$

The corresponding evolution equation in the tangent space is

$$u_i(t+1) = m_i(t) \left\{ \varepsilon u_{i-1}(t) + (1-2\varepsilon)u_i(t) + \varepsilon u_{i+1}(t) \right\}, \quad (2)$$

where $m_i(t) \equiv f'(y_i(t+1))$. From Eq. (2), we see that the last of the above mentioned three effects of the spatial coupling can be isolated and studied separately from the other ones. It is sufficient to assume that the distribution of multipliers is independent of the coupling strength ε and that the $m_i(t)$'s are δ -correlated both in space and time. These

approximations are equivalent to introducing a random-matrix approximation in full analogy with Refs. [4,5].

The first author who investigated the effect of a small coupling on a chaotic dynamics was Daido [6], who studied numerically two coupled maps as well as two continuous-time chaotic oscillators. He also attempted a combined analytical and numerical study to explain the observed behaviour, without however being able to go beyond the prediction of the scaling behaviour.

Later on, the problem of (infinitely many) coupled maps was considered in Ref. [4], by exploiting the analogy with the statistical mechanics of directed polymers in random media. Indeed, Eq. (2) can be also read as the recursive equation for the partition function “ $u_i(t)$ ” of a polymer of length t which grows by adding each new monomer no farther than one site from the last one. A possibly relevant difference between the two problems comes from the “Boltzmann weight” m_i which is necessarily positive in the polymer case (being a probability), while it can be negative in a CML (m_i being the derivative of the map f). This is a first issue that makes the problem (2) more difficult to be treated and it is the reason why previous studies have been restricted to the case of strictly positive multipliers [4,5]. In fact, without entering the mathematical treatment, one can see that if m_i can be either positive or negative, $u_i(t)$ is no longer positive definite and partial cancellations can occur in the iteration of the recursive relation.

The efforts made in [4] to estimate the MLE consisted in developing a mean field analysis on the basis of the equivalence between the MLE in CML and the free-energy in directed polymers. By thus using the approaches developed in [7,8], it was possible to show that the spatial coupling induces an increase of the MLE from the “quenched” average $\Lambda_0 = \langle \log m_i \rangle$ (corresponding to the absence of a spatial coupling) towards the “annealed” average $\Lambda_0 = \ln \langle m_i \rangle$, holding above some critical coupling value. While some features of this scenario were qualitatively confirmed by the numerical simulations (as, e.g., the increase of the MLE), no evidence of the phase transition was actually found. A perturbative technique, developed later on to improve the previous estimates [5] has shown that the transition point slowly shifts towards larger coupling values, possibly disappearing in the asymptotic limit. Nevertheless, the extremely slow convergence of the estimates of the MLE to the values numerically observed, makes a general implementation of this approach not very appealing. Moreover, we should also recall that the analogy with directed polymers does not even allow an exact prediction of the scaling behaviour of the MLE, in so far as it indicates the existence of an additional, extremely weak, dependence on the coupling strength which seems to be absent in the outcome of direct numerical simulations.

It is also worth recalling the analogy between the behaviour of the MLE and the evolution of rough interfaces. By interpreting the logarithm of (the amplitude of) the perturbation as the height of an abstract interface, the Lyapunov exponent becomes equivalent to the velocity of one such interface [9,10]. However, this analogy is of no utility in the present case, since the deviation of the MLE from the uncoupled limit cannot be determined by studying the corresponding Kardar-Parisi-Zhang (KPZ) equation as already remarked in [5]. In a sense, the MLE corrections are connected to non-trivial deviations from a KPZ behaviour over short temporal and spatial scales.

In the present paper we derive approximate but analytical expression for the MLE, by mapping the original problem onto that of a chain of continuous-time, nonlinear Langevin

equations. Such a set of equation is then reduced to a single stochastic equation whose solution yields an expression for the MLE that is in good agreement with direct numericals simulations. As the whole approach does not make use of the specific structure of the initial equations, we are rather confident that it can be repeated for other types of couplings, the only difference being presumably the structure of the deterministic force in the final stochastic equation. Moreover, we would like to point out that the mapping onto continuous-time equations indicates that the initial discreteness of the time variable is not a distinctive feature and we can imagine that a similar approach works also in the case of coupled chaotic oscillators. Our hope is reinforced by the observation that some equations obtained in the present framework can be derived also in the case of two weakly coupled differential equations [11].

The paper is organized as follows. In Sec. II, we briefly introduce the problem and some notations. In Sec. III we discuss the properties of tangent dynamics in the case of strictly positive multipliers: the analytical treatment is followed by a comparison with the numerical results. In Sect. IV we extend the analytical treatment to the case of multipliers with random signs. Finally, in Sect. V we summarize the main results and comment about the still open problems. The two appendices are devoted to the small-noise limit in the case of strictly positive multipliers and, respectively, to the small coupling regime in the general case of random signs.

II. PRELIMINARY TREATMENT

In this section, we formulate the problem of computing the MLE under the assumption of a small coupling strength. The first step consists in introducing the ratio between the perturbation amplitude in two consecutive site,

$$R_j(t) \equiv u_j/u_{j-1} \quad (3)$$

which allows writing Eq. (2) as

$$\ln \left| \frac{u_i(t+1)}{u_i(t)} \right| = \ln |m_i(t)| + \ln \left| 1 - 2\varepsilon + \varepsilon R_{i+1}(t) + \frac{\varepsilon}{R_i(t)} \right|, \quad (4)$$

where the average of the l.h.s. is nothing but the MLE $\Lambda(\varepsilon)$, while the r.h.s. is naturally expressed as the sum of the 0-coupling value plus the correction term induced by spatial interactions.

A more convenient way of writing the Lyapunov exponent is obtained by transforming the smallness parameter as

$$\gamma \equiv \varepsilon/(1 - 2\varepsilon), \quad (5)$$

which leads to

$$\Lambda(\varepsilon) = \left\langle \ln \left| \frac{u_i(t+1)}{u_i(t)} \right| \right\rangle = \Lambda(0) + \ln(1 - 2\varepsilon) + \delta\Lambda(\gamma), \quad (6)$$

where the Lyapunov correction is split into two parts, a multiplier-independent term and a non-trivial contribution

$$\delta\Lambda(\gamma) = \left\langle \ln \left| 1 + \gamma R_{i+1} + \frac{\gamma}{R_i} \right| \right\rangle, \quad (7)$$

where $\langle \cdot \rangle$ represents the time-average along the trajectory generated by Eq.(1) or, equivalently, the ensemble-average if ergodicity holds.

Eq. (7) tells us that the determination of the MLE requires the prior knowledge of the invariant measure of the stochastic process $R_i(t)$ on two consecutive sites. By expanding the logarithm in powers of γ , the correction to the MLE can be expressed in terms of all the momenta of the probability distribution,

$$\delta\Lambda(\gamma) = - \sum_{j=1}^{\infty} \sum_{m=1}^j \frac{(j-1)!(-\gamma)^j}{m!(j-m)!} \left\langle R_{i+1}^m R_i^{j-m} \right\rangle. \quad (8)$$

It is, therefore, necessary to formulate the dynamical equation in terms of the variable R_i . This can be easily done from Eqs. (3,4)

$$R_i(t+1) = \mu_i(t) \frac{R_i(t) + \gamma R_i(t) R_{i+1}(t) + \gamma}{1 + \gamma R_i(t) + \gamma/R_{i-1}(t)}. \quad (9)$$

where we have introduced the stochastic process

$$\mu_i(t) \equiv m_i(t)/m_{i-1}(t) \quad (10)$$

whose geometric average is equal to 1, μ_i being the ratio of two i.i.d. processes.

III. POSITIVE MULTIPLIERS

We first consider strictly positive multipliers, while the more general case is addressed in the following section. In fact, while the two cases require a somehow different treatment, a discussion of the former problem allows introducing several tools that turn out to be useful also in the latter context.

A. Theory

If the μ_i 's are positive definite, the ratios R_i 's remain positive whenever initialized as such. This allows introducing the variable $w_i = \ln R_i$ without the need of dealing with the sign of R_i . The introduction of w_i is convenient in that it transforms the original problem into a stochastic process with additive rather than multiplicative noise. With no restriction other than the positiveness of the multipliers, we obtain

$$w_i(t+1) - w_i(t) = \ln \mu_i(t) + \ln \left\{ 1 + \gamma e^{w_{i+1}(t)} + \gamma e^{-w_i(t)} \right\} - \ln \left\{ 1 + \gamma e^{w_i(t)} + \gamma e^{-w_{i-1}(t)} \right\}. \quad (11)$$

In the limit of small γ , the arguments of the logarithms differ slightly from 1, provided that w_i does not deviate too much from 0. Under this approximation (that can be checked a posteriori), we can expand the logarithms, retaining the leading terms and thereby introducing

a continuous-time representation (because of the smallness of the deterministic variations). One obtains

$$\dot{w}_i = -2\gamma \sinh(w_i) + \gamma \left(e^{w_{i+1}} - e^{-w_{i-1}} \right) + \xi_i(t) \quad (12)$$

where $\xi_i \equiv \ln \mu_i$, has zero average and correlation function,

$$\langle \xi_i(t) \xi_j(t') \rangle = 4\sigma^2 \delta(t - t') (\delta_{i,j} - \frac{1}{2} \delta_{i \pm 1, j}) \quad (13)$$

where σ^2 is the variance of the logarithm of the multiplier m_i and there is a factor 4 (instead of the usual 2) since the noise term is the “sum” of two i.i.d. processes ($\xi_i = \ln m_i - \ln m_{i-1}$). Spatial correlations of the stochastic forces are all zero except those of neighbouring sites, a feature induced by the very definition of ξ_i as the sum of two processes in neighbouring sites.

It is important to notice that the only parameter of the sequence of multipliers which eventually contributes to the correction of the MLE is precisely the amplitude of the fluctuations.

Eq. (12) represents a chain of coupled Langevin equations describing the evolution of interacting “particles”. Even without solving the model, it is possible to realize that only one parameter suffices to describe the scaling behaviour of the Lyapunov exponent, the rescaled smallness parameter

$$g = \gamma/\sigma^2, \quad (14)$$

which can also be interpreted as the inverse effective diffusion constant. In fact, the factor γ in front of the deterministic forces can be eliminated by properly scaling the time units.

In the next sub-section, we investigate numerically the validity of this prediction by computing the Lyapunov exponent for different values of σ and γ and thereby checking whether the data collapses onto a single curve.

The evaluation of $\delta\Lambda(\gamma)$ requires finding the invariant measure for the whole set of stochastic equations (12). This is still a difficult problem, since the deterministic forces do not follow from a potential and, therefore, the corresponding Fokker-Planck equation cannot be straightforwardly solved. In particular, it is interesting to notice that, although we are working in the limit of weakly coupled maps, the “particles” are not weakly interacting. This is the most serious difficulty towards a perturbative treatment of the problem. Nevertheless, we are going to see that this infinite set of stochastic equations can be effectively approximated by a single Langevin equation.

Formally speaking, the probability distribution $P_L(w_1, \dots, w_L; t)$ satisfies the Fokker-Planck equation

$$\frac{\partial P_L}{\partial t} = - \sum_{i=1}^L \frac{\partial}{\partial w_i} \left\{ F(w_i) P_L + \Phi(w_{i+1}, w_{i-1}) P_L \right\} + \frac{1}{2} \sum_{i,j=1}^L \mathcal{D}_{i,j} \frac{\partial^2 P_L}{\partial w_i \partial w_j} \quad (15)$$

where

$$F(w_i) = -2\gamma \sinh(w_i) \quad (16)$$

is the single-particle force (see Eq. (12), $\Phi(w_{i+1}, w_{i-1}) = -2\gamma(e^{w_{i+1}} - e^{-w_{i-1}})$ is the coupling term and $\mathcal{D}_{i,j}$ are the diffusion coefficients as from (13).

Let us now introduce the single-particle distribution $P(w_i)$ by integrating over all the other $L - 1$ degrees of freedom

$$P(w_i, t) = \int \prod_{j \neq i} dw_j P_L(w_1, \dots, w_L; t).$$

The corresponding equation can be directly derived from Eq. (15),

$$\begin{aligned} \frac{\partial P}{\partial t} = & -\frac{\partial}{\partial w_i} \{F(w_i)P\} + 2\sigma^2 \frac{\partial^2 P}{\partial w_i^2} + \\ & -\gamma \frac{\partial}{\partial w_i} \left\{ \int dw_{i+1} P_2(w_i, w_{i+1}) e^{w_{i+1}} - \int dw_{i-1} P_2(w_{i-1}, w_i) e^{-w_{i-1}} \right\} \end{aligned} \quad (17)$$

Eq. (17) is not closed since it involves the unknown two-body distribution P_2 . The above is indeed the first of a hierarchy of equations involving probability distributions of increasing order. The simplest approximation to close the system consists in truncating the hierarchy at the lowest level by assuming a perfect factorization, $P_2(x, y) = P(x)P(y)$. This is the standard mean-field approach which leads to the closed Fokker-Planck equation

$$\frac{\partial P}{\partial t} = -\frac{\partial}{\partial w} \{F(w)P\} + 2\sigma^2 \frac{\partial^2 P}{\partial w^2}, \quad (18)$$

since the symmetry of the distribution ($P(w) = P(-w)$) implies that the coupling terms cancel each other.

The Fokker-Planck equation (18) corresponds to the single-particle Langevin equation

$$\dot{w} = F(w) + \xi(t), \quad (19)$$

where we have dropped the by now irrelevant spatial dependence.

It is instructive to test the validity of the above approximation in the limit of large g values, when the forces can be linearized and an analytic solution can be obtained for the entire chain of Langevin equations. For the sake of readability, the discussion of this technical problem is presented separately in the first Appendix. The main result of this analysis is that the approximation (19) is exact! The stationary probability distribution of Eq. (18) is equal to the projection of the many-particle distribution for the whole chain. However, one cannot expect that the same holds true also for finite g values, when nonlinearities come into play.

Let us therefore discuss a possible line of thought to go beyond the approximation (19). It is first important to recognize the special nature of the noise ξ , which keeps $W(t) = \sum_i w_i(t)$ constantly equal to zero. Indeed, W is nothing but the logarithm of the ratio between the amplitude of the perturbation in the first and the last site. If periodic boundary conditions are assumed, as we do, this implies that $W(t) = 0$. A simple way to satisfy this constraint is to assume $w_i = -w_{i-1}$. By substituting this extreme assumption into Eq. (12), we obtain again a Langevin equation with the same force as in Eq. (16) but a different factor. It is therefore reasonable to conjecture that, in general, the effective force strength depends on g , thus writing (in rescaled time-units)

$$F(w) = -2\alpha(g) \sinh(w) \quad (20)$$

where α is a renormalization factor to be determined with some self-consistency argument. As we have not found any sensible way to do so, we limit ourselves to investigate numerically its possible dependence on g .

The stationary distribution w is obtained by solving the Fokker-Planck equation (18),

$$P(w) = \mathcal{C} \exp[-\alpha\gamma/\sigma^2 \cosh(w)], \quad (21)$$

where the normalization constant $\mathcal{C} = 2K_0(\alpha\gamma/\sigma^2)$ is expressed in terms of the zeroth-order modified Bessel function [12,13]

$$K_\nu(x) = \int_{-\infty}^{\infty} dt \exp\{-x \cosh(t) \pm \nu t\}.$$

By substituting the definition of w ($w = \ln R$) in Eq. (8), and assuming $\langle w_i w_{i-1} \rangle = 0$ (an hypothesis accurately confirmed by direct numerical simulations), we finally obtain

$$\delta\Lambda(\gamma) = - \sum_{j=1}^{\infty} \sum_{m=1}^j \frac{(j-1)!(-\gamma)^j}{m!(j-m)!} \frac{K_m(2g)K_{j-m}(2g)}{K_0(2g)^2} \quad (22)$$

As γ is assumed to be small, we can safely retain only the first two terms of the series (22), obtaining

$$\delta\Lambda(\gamma) = 2\gamma \frac{K_1(2g)}{K_0(2g)} \quad (23)$$

which represents the (approximate) perturbative expression for the correction to the MLE in the limit of small coupling.

First of all, it is instructive to investigate the limit $g \ll 1$, by using the asymptotic expression of the functions $K_\nu(y)$. Since

$$K_0(y) \sim -\ln(y/2) \quad , \quad K_1(y) \sim \frac{1}{y}, \quad (24)$$

we find that

$$\delta\Lambda(\gamma) \sim \frac{\sigma^2}{\ln(1/g)} \quad (25)$$

This equation represents a relevant improvement over the previous results. First of all, it is in agreement with numerical simulations which do not give evidence of a $\ln|\ln g|$ correction in the numerator, as instead predicted by the statistical-mechanics treatment based on the analogy with directed polymers [5].

A second and more important remark concerns the dependence on the “noise” strength which is explicitly determined. Previously it was only clear that the correction to the MLE must vanish if there is no multifractality (no multiplier fluctuations) but the dependence on σ was not known.

B. Numerical results

The theoretical analysis performed in the previous section is mainly based on a perturbative approach. Moreover, it involves a nontrivial transformation of a set of coupled Langevin equations to a single effective Langevin equation in a limit where the coupling is not negligible. Therefore, a comparison of the theoretical predictions with direct numerical simulations is worth especially to check the validity of the dynamical mean-field approximation that is behind this last step.

We have decided to test the theoretical results by using two different probability densities: A) uniform distribution of multipliers m_i within the interval $[e^a(1 - \Delta_1/2), e^a(1 + \Delta_1/2)]$; B) uniform distribution of the logarithms of the m_i within $[a - \Delta_2/2, a + \Delta_2/2]$. The corresponding Lyapunov exponents in the uncoupled limit ($\varepsilon = 0$) are

$$\Lambda_A(0) = a - 1 + \frac{1}{\Delta_1} \left\{ \left(1 + \frac{\Delta_1}{2}\right) \ln \left(1 + \frac{\Delta_1}{2}\right) - \left(1 - \frac{\Delta_1}{2}\right) \ln \left(1 - \frac{\Delta_1}{2}\right) \right\}$$

$$\Lambda_B(0) = a,$$

while the variances of $\ln m_i(t)$ are

$$\sigma_A^2 = 1 - \frac{1}{\Delta_1^2} \left(1 - \frac{\Delta_1^2}{4}\right) \ln^2 \left(\frac{1 + \Delta_1/2}{1 - \Delta_1/2}\right) \quad (26)$$

$$\sigma_B^2 = \frac{\Delta_2^2}{12}. \quad (27)$$

We start from testing the predictions for the shape of the probability distribution of w . Two meaningful examples are reported in Fig. 1, where the open circles refer to the histograms, while the solid line is the theoretical result (Eq. (21) with α set equal to 1). Let us first comment about the qualitative shape of the distribution. In the limit of large g , the noise is almost negligible and therefore, the phase point is expected not to deviate significantly from the stable fixed point $w = 0$. It is therefore possible to linearize the equation, finding a Gaussian distribution. This is precisely the message contained in Fig. 1a, which refers to $g = 2.4$. In the limit of small g instead, it is the force that can be neglected except when the deviations are large. Since the attracting force grows very rapidly (exponentially), it makes sense to replace the corresponding potential with a flat well with infinitely high barriers placed where the deterministic force is of the same order as the stochastic one. In this picture, one expects that the probability distribution is just a uniform distribution in a finite interval (this is the kind of argument introduced in [4] to predict the scaling behaviour in this regime). This scenario can be qualitatively recognized in Fig. 1b, which refers to $g = 0.021$.

Next, let us comment about the quantitative agreement between the theoretical expectations and the numerical findings. In Fig. 1a, there is an almost perfect agreement. This is a first encouraging result, since it indicates that even for not too large a value of g , the effective force strength remains equal to 2γ with no renormalization. Some deviations are instead observed in Fig. 1b, where the theoretical curve is slightly more peaked, suggesting that the effective force is smaller than expected. A simple way to determine α is by fitting

the numerical data. In the first case we find that $\alpha = 0.97$ confirming the first qualitative impression; in the second case $\alpha = 0.75$ indicating stronger but not significative deviations from the linear regime. The curve corresponding to the fitted value of α is reported in Fig. 1b as a dashed line. The residual, small, deviations with respect to the numerical data indicate that the reduction of the original model to a single stochastic equation with the effective force (20) is indeed a strategy that is worth being pursued.

All the other cases that we have tested reveal the same scenario. Altogether, we can summarize stating that the major discrepancy between numerics and theoretical prediction is contained in the renormalization factor α which is assumed to be equal to 1 in our treatment but turns out to depend on g ; nevertheless it is never smaller than 0.7.

Since the aim of the present paper is to study the corrections to the MLE induced by the spatial coupling, let us now discuss this issue. In order to assess the quality of our theoretical predictions, we performed numerical iterations of Eq. (2) computing the MLE with the well known algorithm [14]. Simulations have been carried out on 500-site lattices, imposing periodic boundary conditions. In every simulation the first 500 iterations have been discarded to avoid any bias effect due to initial conditions. Tests made with different lattice lengths indicate that finite-size effects are always much smaller than the deviation from the theoretical predictions.

The first nice result is provided by Fig. 2a. The data is plotted in order to emphasize the existence of only one relevant parameter, g . Indeed, the good data collapse (all data align along the same curve irrespective of the value of γ , σ or the type of probability distribution) represents a further confirmation of our theoretical analysis. Moreover, the nice agreement of the numerical data with the theoretical expression (23) (see the solid line in Fig. 2a) over a wide range of values of the effective coupling testifies to the accuracy of the approximations introduced in the first part of this section.

However, there is a better way to emphasize the differences between theory and numerics. In fact, the limit $g \rightarrow \infty$ corresponds to negligible noise, i.e. to a regime where the MLE Lyapunov exponent is unaffected by the presence of spatial coupling as shown in [15]. It is therefore convenient to look at the behaviour of the whole deviation of the Lyapunov exponent $\Delta\Lambda = \delta\Lambda - 2\gamma$, which again exhibits the same scaling behaviour as seen by dividing this expression by σ^2 and using Eq. (25)

$$\frac{\Delta\Lambda}{\sigma^2} = 2g \left(\frac{K_1(2g)}{K_0(2g)} - 1 \right). \quad (28)$$

The data plotted this way are reported in Fig. 2b. We clearly see that the trivial correction term -2γ cancels almost exactly the growth exhibited by $\delta\Lambda$ for large g -values allowing for a more stringent test of the theoretical prediction. We can now see that the absolute difference is not larger than 0.05 and it could be greatly reduced by suitably shifting the theoretical curve (i.e. by rescaling g by approximately a factor 2) as shown by looking at the dashed curve. However, in the absence of theoretical arguments, this observation cannot be considered more than a hint for future considerations.

IV. THE GENERAL CASE

A. Theory

In this section, we account for sign fluctuations as well. In order to keep the theoretical treatment as simple as possible, we shall assume that the sign is a δ -correlated stochastic process independent of the modulus, so that the average factorizes as

$$\langle m_i \rangle = (p - q) \langle |m_i| \rangle,$$

where p (q) is the probability that m_i is positive (negative). The major difference with respect to the previous case is that the ratio R_i can also assume negative as well as positive values. It is therefore more convenient to work with R_i instead of introducing its logarithm which would require introducing absolute values and thus two different variables to account for the dynamics in the positive as well as in the negative range of R_i values.

We have learned in the previous section that neglecting the coupling with the neighbouring sites provides a good approximation of the probability distribution and thereby of the MLE. Let us therefore neglect the dependence on R_{i+1} and R_{i-1} in Eq. (9). As a result, we obtain the one dimensional mapping

$$R(t+1) = \mu(t) \frac{R(t) + \gamma}{1 + \gamma R(t)}, \quad (29)$$

where, for the sake of simplicity, we have removed the now irrelevant site dependence. In the continuous-time approximation, the above would be exactly the equation that has allowed an approximate analytical treatment in the case of positive signs. Mapping (29) possesses two remarkable symmetry properties: the evolution is invariant under the transformation $R \rightarrow 1/R$, since the stochastic process μ turns out to be invariant under the same transformation $\mu \rightarrow 1/\mu$ (it is sufficient to look at its definition). This is the same symmetry as that one discovered in the previous section when we have found that the potential $V(w)$ is an even function of w . As a consequence, we can restrict our analysis to the interval $[-1, 1]$.

The second symmetry has much more serious implications. We can see that the mapping (29) is also invariant under time-reversal. More precisely, if we express $R(t)$ as a function of $R(t+1)$ we find the same functional form of mapping (29), provided that the changes of variables $S : R(t+1) \rightarrow -R(t+1)/\mu(t)$ and $\mu \rightarrow 1/\mu$ are introduced as well. As the transformation S is an involution (i.e., $S^2 = Id$), we can state that mapping (29) is invariant under time-reversal. Therefore, we seem to be in the presence of a contradiction, as this property holds also for strictly positive multipliers, when it is clear that there is an attractor (the point $w = 0$, i.e. $R = 1$), since time-reversibility hints at a lack of attractors! Indeed, there is no contradiction, since time-reversal symmetry is broken in the case of strictly positive multipliers. In fact, invariance of the mapping implies only that a given solution can be neither stable nor unstable, if it is itself invariant under the involution S . However, this is not the case for the fixed point $R = 1$ (in the absence of noise, i.e. for $\mu = 1$) which is mapped by S onto $R = -1$, so that we can only conclude that if $R = 1$ is stable, then $R = -1$ must be unstable (as it is indeed the case). In other words, positive values of R are characterized by a contracting dynamics towards $R = 1$, while negative values depart from -1 . If the multipliers are strictly positive, negative R -values cannot be asymptotically observed as they lie in the repelling part of the phase-space and the previous treatment in terms of a Langevin equation with an attracting force makes perfectly sense.

On the other hand, if the multipliers can assume both signs, the dynamical rule allows visiting interchangeably the positive as well as the negative region. In principle, it is still possible to have, on the average, a global contraction provided that a longer time is spent in the positive region. Actually, this is the assumption more or less implicitly made in Ref. [16], where it was conjectured that no qualitative changes are expected when positive and negative multipliers come into play except for the degenerate case $p = q = 1/2$. We see below that even if the scaling behaviour in the limit of vanishing coupling is unaffected, this is not true and it indeed requires introducing a different scaling parameter.

The most effective way we have found to analyse mapping (29) is by exploiting another property: the possibility to transfer the change of sign of μ to γ . With this trick, the change of sign in Eq. (29) can be effectively treated perturbatively being γ a small parameter. More precisely, if $\mu(t)$ happens to be negative, we can assume it to remain nevertheless positive and perform the next iteration with $-R(t+1)$. It can then be seen that the resulting expression is the same as the original one after changing the sign of γ and of $\mu(t+1)$. Now, irrespective of the sign of $-\mu(t+1)$, we assume it to be positive and transfer its sign to the next value of γ . In other words, we can iterate the mapping

$$R(t+1) = |\mu(t)| \frac{R(t) + \gamma(t)}{1 + \gamma(t)R(t)}, \quad (30)$$

where the sign of $\gamma(t)$ is that of $\prod_{s=1}^{t-1} \mu(s)$. We can immediately see that even if μ is on the average more positive than negative (or vice versa), the sign of γ has no preference, since it simply depends on the parity of the number of sign changes. It is because of this reason that fluctuating multipliers are qualitatively different from strictly positive ones: even an asymmetry in the signs (a preference, say, for the positive values) implies that the unstable and stable region (positive and negative values of R in the initial representation) are equally visited.

The dichotomic structure of the noise $\gamma(t)$ allows expressing the stochastic map as the sum of a net drift plus a zero-average fluctuating term. Indeed, by calling $F_+(R)$ and $F_-(R)$ the l.h.s. of Eq. (30) whenever γ is positive, respectively, negative, we can write

$$R(t+1) = \frac{1}{2} \left\{ F_+(R(t)) + F_-(R(t)) \right\} + \frac{\delta(t)}{2} \left\{ F_+(R(t)) - F_-(R(t)) \right\} \quad (31)$$

where $\delta(t)$ is again a dichotomic noise with entries equal to ± 1 . More specifically, we obtain

$$R(t+1) = \frac{|\mu|}{2} \frac{(1 - \gamma^2)R}{1 - \gamma^2 R^2} + |\mu| \delta(t) \frac{\gamma(1 - R^2)}{1 - \gamma^2 R^2}. \quad (32)$$

In order to obtain an analytic expression for the probability density of R , it is convenient to turn this equation into a continuous-time model.

This is possible at the expense of assuming that the modulus fluctuations of μ are small, i.e. by writing $|\mu| = 1 + \nu$, and by then expanding the r.h.s. in (32). By retaining terms up to second order, we obtain

$$\dot{R} = \gamma^2 R(R^2 - 1) + (\nu + \bar{\sigma}^2/2)R + \delta(t)\nu\gamma(1 - R^2), \quad (33)$$

where $\bar{\sigma}^2$ is the variance of ν .

Before going on, it is important to notice that the above equation must be interpreted in the Ito sense as it arises from a discrete time stochastic process with δ -correlated noise [17] (this problem did not arise in the previous section, since we were dealing with an additive noise). Moreover, it is instructive to notice that the drift term in Eq. (33) is purely induced by noise: it arises from the inhomogeneity of the stochastic process. This represents a direct confirmation that contraction and expansions processes tend to compensate each other as already anticipated in the beginning of this Section.

If the time variable is rescaled by a factor $\bar{\sigma}^2$, it is immediately recognized that the dynamics of R depends on just one parameter

$$G = \frac{\gamma}{\bar{\sigma}}, \quad (34)$$

which is again a ratio between coupling strength and multiplier fluctuations. However, there is an important difference with the parameter $g = \gamma/\sigma^2$ introduced in the previous case, as it is seen by noticing that in the small $\bar{\sigma}$ limit, the equality

$$\bar{\sigma} = \sqrt{2}\sigma \quad (35)$$

holds. Apart from the irrelevant numerical factor, it turns out that, in the general case, the r.m.s. rather than the standard deviation enters as a measure of multiplier fluctuations.

The Fokker-Planck equation corresponding to the Langevin process (33) in rescaled time units reads as

$$\frac{\partial P}{\partial t} = -\frac{\partial}{\partial R}(AP) + \frac{1}{2}\frac{\partial^2}{\partial R^2}(BP) \quad (36)$$

where

$$A(R) = -G^2 R(1 - R^2) + R/2 \quad (37)$$

is the drift term, while

$$B(R) = R^2 + G^2(1 - R^2)^2 \quad (38)$$

is the diffusion coefficient. Since $4A(R) = dB/dR$, the stationary solution is

$$P(R) = \frac{N(G)}{\sqrt{G^2(1 - R^2)^2 + R^2}} \quad (39)$$

where $N(G)$ is the normalization constant discussed in Appendix B.

An expression for the Lyapunov exponent can be obtained from Eq. (7), by integrating over the above determined probability distribution. Unfortunately, there is a crucial difference with the previous case: we cannot simply expand the logarithm in powers of γ , since this leads to computing the first moment of $P(R)$ which is already a diverging quantity ($P(R)$ decays to zero as slowly as $1/R^2$). Obviously, this is only a numerical artifact: the average of the logarithm itself is still well defined and has a finite value.

Nevertheless, this is an indication that we must be much more cautious in performing power expansions. In particular, this difficulty prevents obtaining a general analytical expression analogous to that one obtained in the previous section in terms of modified Bessel

functions. In this case, even obtaining an expression in the limiting case of small G requires a rather laborious work. In Appendix B we show that one can eventually show that the non-trivial deviation with respect to the uncoupled limit is given by

$$\delta\Lambda = \frac{3\sigma^2}{2\ln(1/G)}, \quad (40)$$

Therefore, we see that also in the general case of positive/negative signs, the leading dependence on ε is of the type $1/\ln\varepsilon$, as numerically observed. What is different is the dependence on the multiplier fluctuations as testified by the presence of the parameter G rather than g .

B. Numerical results

The first meaningful test of the analytical approach devised in the previous sub-section concerns the probability distribution $P(R)$. In Fig. 3 we report the outcome of a numerical experiment in doubly-logarithmic scales (see the full dots). This allows seeing a crossover from an initial decay as $1/R$ to the asymptotic decay $1/R^2$, which represents the first qualitative confirmation of the theoretical predictions. However, the agreement with expression (39) (represented by the dashed line) is more than just qualitative. In fact, besides noticing the almost perfect overlap, one should also remember that the only parameter entering Eq. (39), i.e. G , has not been fitted, but independently determined from the fluctuations of the local multipliers. As a last remark, we would like to point out that the good agreement is not totally obvious a priori at least for the reason that the reduction from a set of coupled stochastic equations to a single equation is not completely under control.

Moreover, it is instructive to compare the shape of this distribution with the results predicted by the theory for strictly positive multipliers. By expressing the probability density of Eq. (21) in terms of R , we find an exponential tail ($P(R) \simeq \exp(-gR)/R$). The power law observed in Fig. 3 is also, therefore, an evidence of a clear difference between the two regimes.

Finally, let us look at the deviations of the MLE plotted versus the scaling parameter G . The data reported in Fig. 4 have been obtained for different noise amplitudes and either $\varepsilon = 10^{-3}$ (diamonds) or $\varepsilon = 10^{-5}$ (circles). It is clearly seen that, $\delta\Lambda \ln G/\sigma^2$ is constant, independently of the value of G . This confirms the scaling behaviour predicted by Eq. (40). A more quantitative check can be made by comparing the actual value of $\delta\Lambda \ln G/\sigma^2$ (about $1.1 \approx 1.2$ in direct simulations) with the theoretical prediction (1.5). We believe that the deviation is to be ascribed to the approximation made in reducing the set of coupled stochastic equations to a single Langevin equation.

V. CONCLUSIONS AND PERSPECTIVES

In this paper we have developed a theoretical method that is able to explain not only the scaling behaviour of the maximum Lyapunov exponent for a CML in the small coupling limit, but provides a quantitative estimation of its deviations from the uncoupled case. This was still lacking even in the relatively simple case of strictly positive multipliers. However, we have gone further, developing a treatment also for multipliers with random signs. In

both cases we have found that the correction to the maximum Lyapunov exponent induced by local interactions actually depends on a single scaling parameter which is nothing but the coupling strength rescaled by the “amplitude” of multiplier fluctuations. However, the scaling parameter is significantly different in the two cases: for strictly positive multipliers, the fluctuation “amplitude” is the mean square deviation σ^2 (see the definition of g - Eq. (14)), while in the case of random signs, the “amplitude” is the r.m.s. deviation (see the definition of G - Eq. (34)).

Important differences can also be detected in the probability distribution of the local ratios R_i of the perturbation amplitude in two adjacent sites: in the case of fluctuating signs there are long tails characterized by a power law decay.

Among the still open problems, there is certainly the exigence of a more rigorous procedure to solve the set of coupled Langevin equations. In fact, while the derivation of the set of coupled stochastic equations is the result of a well controlled perturbative approach, its reduction to a single equation is based on a mean-field approximation whose validity cannot be controlled a priori but only checked a posteriori.

Finally, we want to mention the possibility of extending this approach to the case of weakly coupled attractors, where time is continuous from the very beginning. This is certainly the most stimulating perspective that is also supported by the preliminary observation that the Langevin equation (19) is obtained also in the case of two weakly coupled differential equations [11].

Acknowledgments We thank the Institute of Scientific Interchange (I.S.I.) in Torino, Italy, where this work was started and partly carried on. We are also indebted to J.M. Parrondo for having pointed out the opportunity to adopt the Ito interpretation.

APPENDIX A: LINEAR LIMIT

This Appendix is devoted to the analysis of Eq. (12) in the linear limit,

$$\dot{w}_i = -\gamma(w_{i+1} - 2w_i + w_{i-1}) + \psi_i(t) - \psi_{i-1}(t), \quad (\text{A1})$$

where we have introduced $\psi_k = \ln\{m_k(t)\}$. This is apparently a discretized Edwards-Wilkinson equation [18], but the spatial structure of the noise prevents the onset of any roughening phenomenon (as commented in the main body of the paper).

To solve this equation, it is convenient to perform a spatial Fourier transform, since it leads to a set of uncoupled equations,

$$\dot{w}(k, t) = -2\gamma(1 - \cos(k))w(k, t) + (1 - e^{ik})\psi(k, t), \quad (\text{A2})$$

where $w(k, t)$ is a complex number that can be decomposed into a real and imaginary part ($w(k, t) = x(k, t) + i y(k, t)$), which satisfy the same equation

$$\dot{x}(k, t) = -2\gamma(1 - \cos(k))x(k, t) + \eta(k, t), \quad (\text{A3})$$

where the noise term η is δ -correlated,

$$\langle \eta(t)\eta(t') \rangle = 2\sigma^2 (1 - \cos(k))\delta(t - t'). \quad (\text{A4})$$

Accordingly, all Fourier modes obey the same Gaussian distribution function,

$$P\{w\} \sim \exp\left(-\frac{\gamma(x^2 + y^2)}{2\sigma^2}\right). \quad (\text{A5})$$

The probability distribution of w_i on a single site is easily obtained by summing the independent distributions corresponding to all modes. As a result, the distribution of w_i is also Gaussian and its variance is σ^2 , as if we had neglected the spatial coupling in Eq. (A1).

APPENDIX B: LYAPUNOV CORRECTION

In this Appendix we determine the nontrivial part of the leading correction to the MLE in the general case. We start by computing the normalization constant. It is convenient to exploit the invariance of $P(R)$ under parity change and the transformation $R \rightarrow 1/R$, to express the normalization condition as

$$1 = 4 \int_0^1 dR P(R) = 4N(G) \int_0^1 \frac{dR}{\sqrt{R^2 + G^2(1 - R^2)^2}}. \quad (\text{B1})$$

Since an explicit analytical expression for the above integral does not exist, we shall limit ourselves to studying the small- G limit. One cannot simply expand the denominator, as it gives rise to a non-integrable singularity in $R = 0$. It is, instead, convenient to introduce the variable $x = R/G$. Afterwards, one can expand the integrand in powers of G without encountering undesired divergences. By retaining the leading terms, we find

$$\frac{1}{N} \simeq 4 \int_0^{1/G} \frac{dx}{\sqrt{1 + x^2}} \simeq 4 \ln\left(1/G\right) \quad (\text{B2})$$

From Eqs. (6,4), it turns out that the estimation of $\delta\Lambda$ requires computing the mean value of $L(R_1, R_2) \equiv \ln|1 + \gamma R_1 + \gamma/R_2|$, i.e.

$$\delta\Lambda = \int_{-\infty}^{\infty} \int_{-\infty}^{\infty} dR_1 dR_2 P(R_1) P(R_2) L(R_1, R_2) \quad (\text{B3})$$

Thanks to the equality $L(R_1, R_2) = L(1/R_2, 1/R_1)$ and to the invariance of $P(R)$ under the transformation $R \rightarrow 1/R$, we can write the Lyapunov correction as the sum of three different contributions, namely

$$\begin{aligned} \delta\Lambda &\equiv \delta_1 + \delta_2 + \delta_3 \\ &= \int_{-1}^1 \int_{-1}^1 dR_1 dR_2 P(R_1) P(R_2) \left\{ L(R_1, 1/R_2) + 2L(R_1, R_2) + L(1/R_1, R_2) \right\} \end{aligned} \quad (\text{B4})$$

with an obvious meaning of the new symbols.

In analogy with the computation of the normalization constant, we introduce the variables $x = R_1/G$ and $y = R_2/G$. As a consequence, the expressions for the three contributions write as

$$\delta_1 = N^2 \int_{-1/G}^{1/G} \int_{-1/G}^{1/G} dx dy \frac{\ln |1 + \gamma Gx + \gamma Gy|}{\sqrt{x^2 + (1 - G^2 x^2)^2} \sqrt{y^2 + (1 - G^2 y^2)^2}} \quad (\text{B5})$$

$$\delta_2 = 2N^2 \int_{-1/G}^{1/G} \int_{1/G}^{1/G} dx dy \frac{\ln |1 + \gamma Gx + \gamma/(Gy)|}{\sqrt{x^2 + (1 - G^2 x^2)^2} \sqrt{y^2 + (1 - G^2 y^2)^2}} \quad (\text{B6})$$

$$\delta_3 = N^2 \int_{-1/G}^{1/G} \int_{-1/G}^{1/G} dx dy \frac{\ln |1 + \gamma/(Gx) + \gamma/(Gy)|}{\sqrt{x^2 + (1 - G^2 x^2)^2} \sqrt{y^2 + (1 - G^2 y^2)^2}} \quad (\text{B7})$$

The inequalities $\gamma \ll G \ll 1$ imply that the contributions proportional to γG in the arguments of the logarithms can be neglected so that δ_1 is negligible altogether. Moreover, G can be always neglected in the denominators, so that the leading contribution to the MLE can be determined by just estimating the two integrals

$$\delta_2 = 2N \int_{-1/G}^{1/G} dy \frac{\ln |1 + \bar{\sigma}/y|}{\sqrt{1 + y^2}} \quad (\text{B8})$$

$$\delta_3 = N^2 \int_{-1/G}^{1/G} \int_{-1/G}^{1/G} dx dy \frac{\ln |1 + \bar{\sigma}/x + \bar{\sigma}/y|}{\sqrt{1 + x^2} \sqrt{1 + y^2}} \quad (\text{B9})$$

where we have re-introduced the parameter $\bar{\sigma}$ for later convenience. We start discussing δ_2 ; it cannot be computed by expanding the logarithm as this leads to an unphysical divergence. It is, instead, helpful to split this contribution into two parts

$$\begin{aligned} \delta_2 &= \delta'_2 + \delta''_2 \\ &= 2N \int_{-1/G}^{1/G} dy \frac{\ln |y + \bar{\sigma}|}{\sqrt{1 + y^2}} - 2N \int_{-1/G}^{1/G} dy \frac{\ln |y|}{\sqrt{1 + y^2}} \end{aligned} \quad (\text{B10})$$

The first integral can be estimated by introducing the variable $w = y + \bar{\sigma}$ and thereby expanding the denominator in powers of $\bar{\sigma}$. By retaining terms up to the second order, we find that δ'_2 can be written as

$$\delta'_2 = 2N \int_{-1/G + \bar{\sigma}}^{1/G + \bar{\sigma}} dw \left\{ \frac{\ln |w|}{\sqrt{1 + w^2}} + \bar{\sigma} \frac{w \ln |w|}{(1 + w^2)^{3/2}} + \frac{\bar{\sigma}^2}{2} \frac{w^2 \ln |w|}{(1 + w^2)^{5/2}} (2w^2 - 1) \right\} \quad (\text{B11})$$

By expanding the zeroth-order term around the integral boundaries in powers of $\bar{\sigma}$, we find that it is equal to $-\delta''_2$ plus corrections of the order $\gamma^2 \ln G$. A contribution of the same order is obtained also by integrating the linear term in $\bar{\sigma}$. However, the leading contribution to the MLE comes from the second-order term which, in the small- G limit can be written as

$$\delta_2 = 2N \bar{\sigma}^2 \int_0^\infty dw \frac{\ln w}{(1 + w^2)^{5/2}} (2w^2 - 1). \quad (\text{B12})$$

The integral can be analytically solved and turns out to be equal to 1, so that [19]

$$\delta_2 = 2N(G) \bar{\sigma}^2 = \frac{\bar{\sigma}^2}{2 \ln(1/G)} \quad (\text{B13})$$

The determination of δ_3 in principle requires even more cumbersome calculations, as it involves a double integral. However, formally deriving the expression for δ_3/N^2 with respect to G , we find that, up negligible corrections,

$$\frac{d\delta_3/N^2}{dG} = -\frac{4}{G} \int_{-1/G}^{1/G} dy \frac{\ln|1 + \bar{\sigma}/y|}{\sqrt{1+y^2}}. \quad (\text{B14})$$

As the integral in this expression is exactly the same involved in the definition of δ_2 (see Eq. (B8)), we can write

$$\frac{d\delta_3/N^2}{dG} = -\frac{2\delta_2}{GN} \quad (\text{B15})$$

Upon substituting the expression for δ_2 (see Eq. (B13)), the above equations can be rewritten as

$$\frac{d\delta_3/N^2}{dG} = -\frac{4\bar{\sigma}^2}{G} \quad , \quad (\text{B16})$$

which, after integration, yields

$$\delta_3 = \frac{\bar{\sigma}^2}{4 \ln(1/G)} \quad (\text{B17})$$

In conclusion, we find that

$$\delta\Lambda = \frac{3\sigma^2}{2 \ln(1/G)} \quad , \quad (\text{B18})$$

where we have preferred to introduce the explicit dependence on the physical parameter σ rather than $\bar{\sigma}$.

REFERENCES

- [1] L. Bunimovich and Ya. Sinai, *Nonlinearity* **1**, 491 (1988).
- [2] S. Aubry and R.S. MacKay, *Nonlinearity* **7**, 1623 (1994).
- [3] M.G. Rosenblum, A.S. Pikovski, and J. Kurths, *Phys. Rev. Lett.* **78**, 4193 (1997) and references therein.
- [4] R. Livi, S. Ruffo and A. Politi, *J.Phys A: Math. Gen.* **25**, 4813 (1992).
- [5] F. Cecconi and A. Politi, *Phys. Rev. E* **56** 4998 (1997).
- [6] H. Daido *Prog. Theor. Phys.* **79** 75 (1984); *Phys. Lett.* **110A** 5 (1985)
- [7] B. Derrida and H. Spohn, *J. Stat. Phys.* **51**, 817 (1988).
- [8] J. Cook and B. Derrida, *Europhys. Lett.* **10**(3) 195 (1989); *J. Phys. A* **23** 1523 (1990); *J. Stat. Phys.* **61** 961 (1990).
- [9] A.S. Pikovsky and J. Kurths, *Phys. Rev. E* **49**, 898 (1994).
- [10] A.S. Pikovsky and A. Politi, *Nonlinearity* **11**, 1049 (1994).
- [11] A. Pikovsky, private communication.
- [12] I.S. Gradshteyn and I.M. Ryzhik, "Table of Integrals, Series and Products" (Academic Press Inc.: New York (USA) 1965)
- [13] M. Abramowitz and I.A. Stegun "Handbook of Mathematical Functions" (Dover Publications, Inc., New York (USA))
- [14] G. Benettin, L. Galgani, A. Giorgilli, and J.-M. Strelcyn, *Meccanica* **9**, 21 (1980); I. Shimada and T. Nagashima, *Prog. Theor. Phys.* **61**, 1605 (1979).
- [15] S. Isola, A. Politi, S. Ruffo, and A. Torcini, *Phys. Lett. A* **143**, 365 (1990).
- [16] A. Torcini, R. Livi, A. Politi, and S. Ruffo, *Phys. Rev. Lett.* **78**, 1391 (1997).
- [17] C.W. Gardiner "Handbook of Stochastic Methods" (Springer-Verlag, Berlin Heidelberg (Germany) 1985).
- [18] A.-L. Barábasi and H.E. Stanley *Fractal Concepts in Surface Growth* (Cambridge University Press: Cambridge UK, 1995).
- [19] We have solved it with the help of Maple software package.

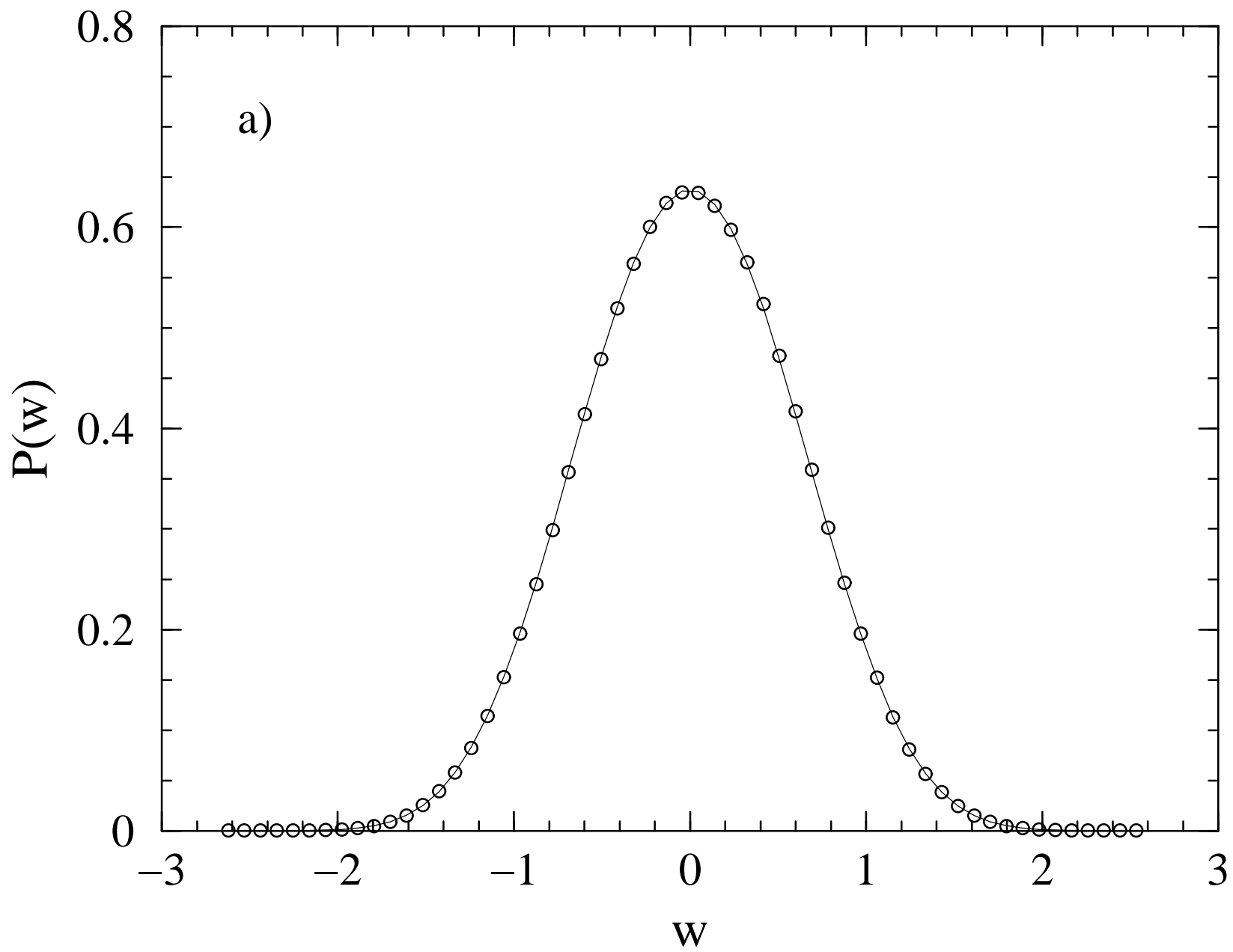
FIGURES

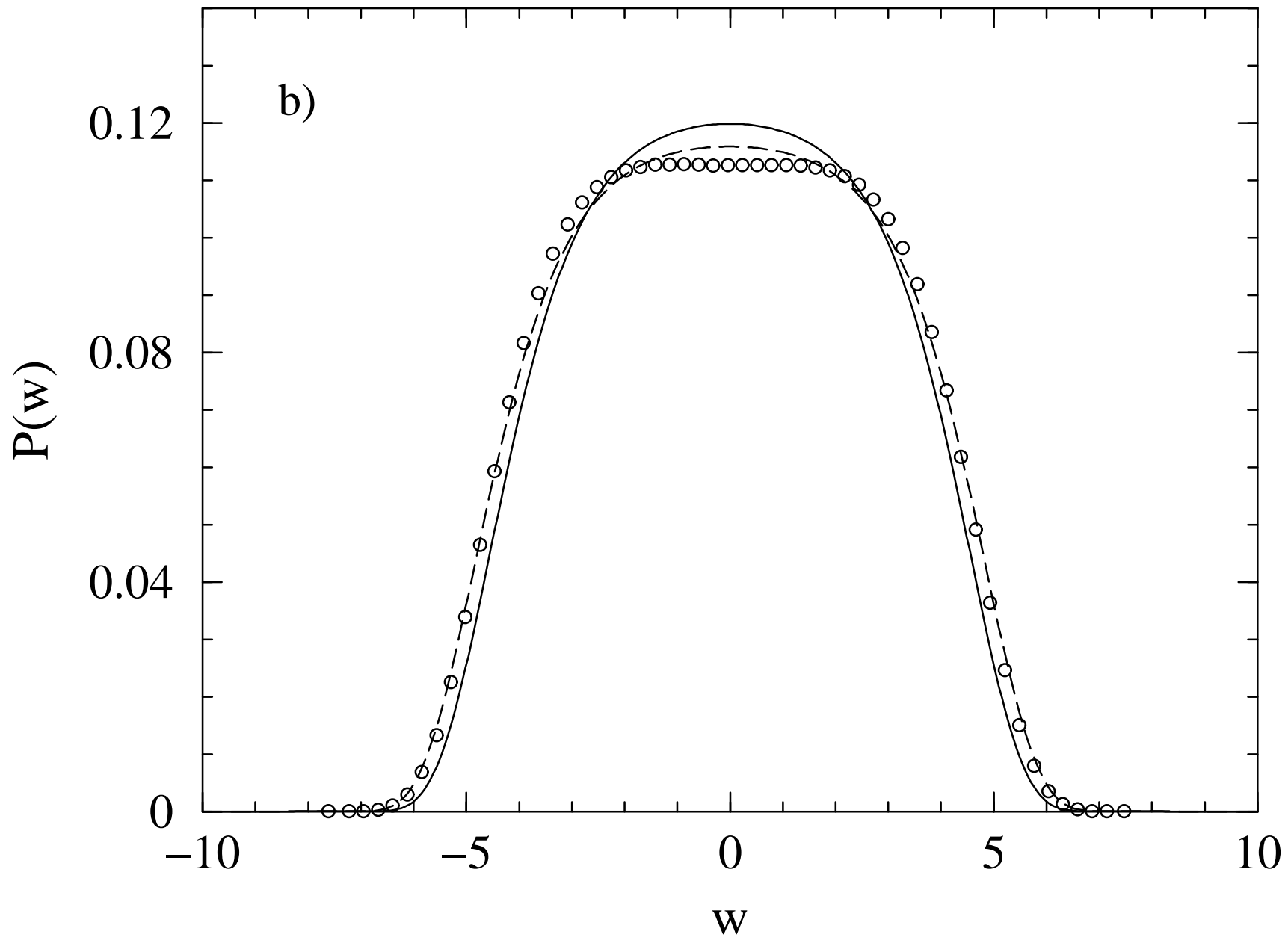
FIG. 1. Probability distribution of w for two different values of g : 2.4 (a) and 0.021 (b). In both cases, circles refer to the numerical histograms, obtained by iterating Eq. (2) for 5×10^7 time-steps (discarding the first 10^3 iterations) on a lattice of $L = 300$ sites. The solid curves correspond to the analytic formula (Eq. (21) with $\alpha = 1$). The dashed curve in (b) is obtained by fitting α which is estimated to be equal to 0.75.

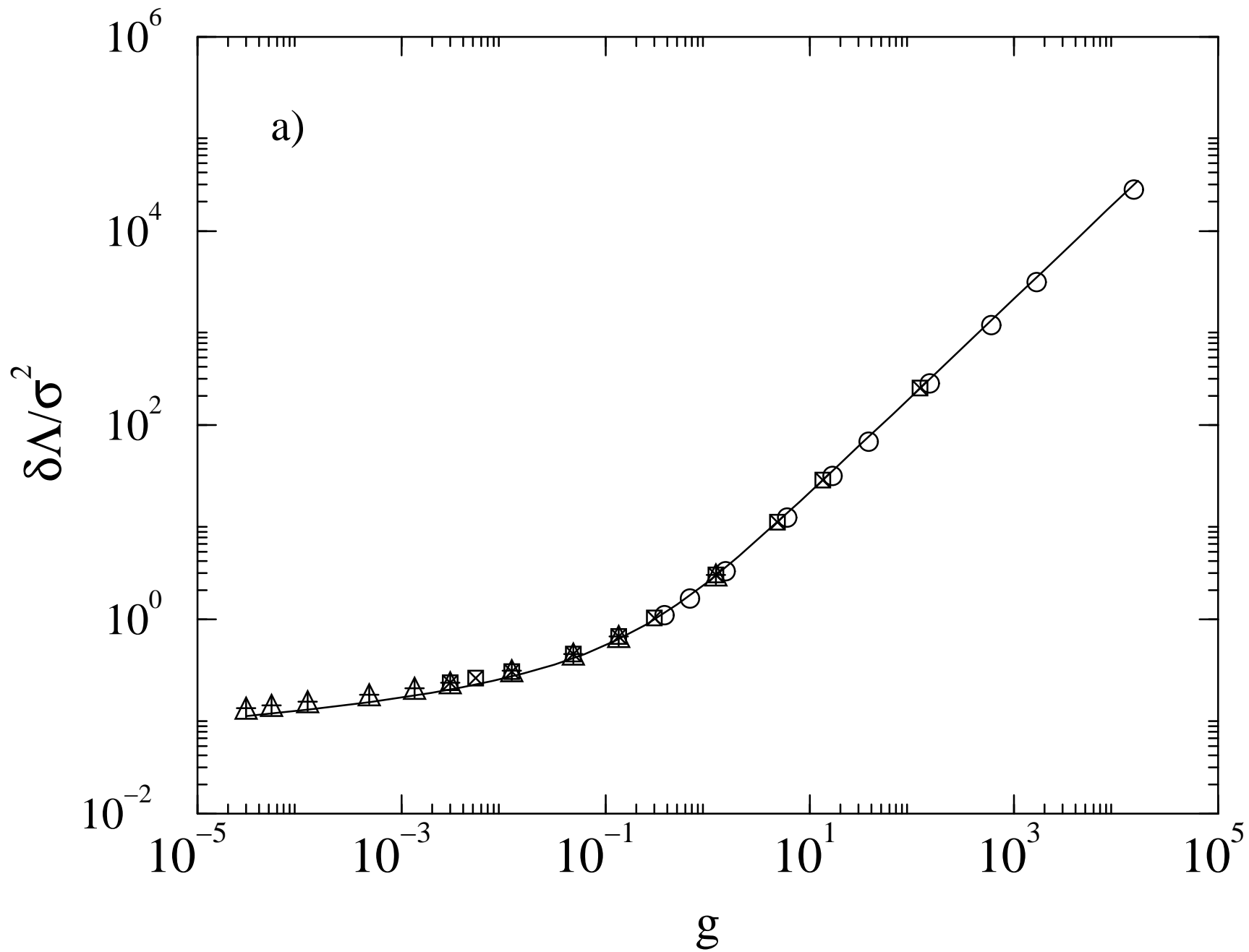
FIG. 2. The Lyapunov exponent versus the scaling parameter g in the case of strictly positive multipliers. The data is obtained by varying ε , σ and for both choices of the probability distribution of the local multipliers (the cases A and B discussed in the text). In a), the shift $\delta\lambda$ defined in Eq. (7) is reported, while in b) the total shift $\Delta\lambda$ (see Eq. (28)) is plotted. The solid curves correspond to the analytic expression. The dashed line in b) is the analytical curve arbitrarily shifted to show that a “renormalization” of the scaling parameter could account for the remaining discrepancy with numerical data.

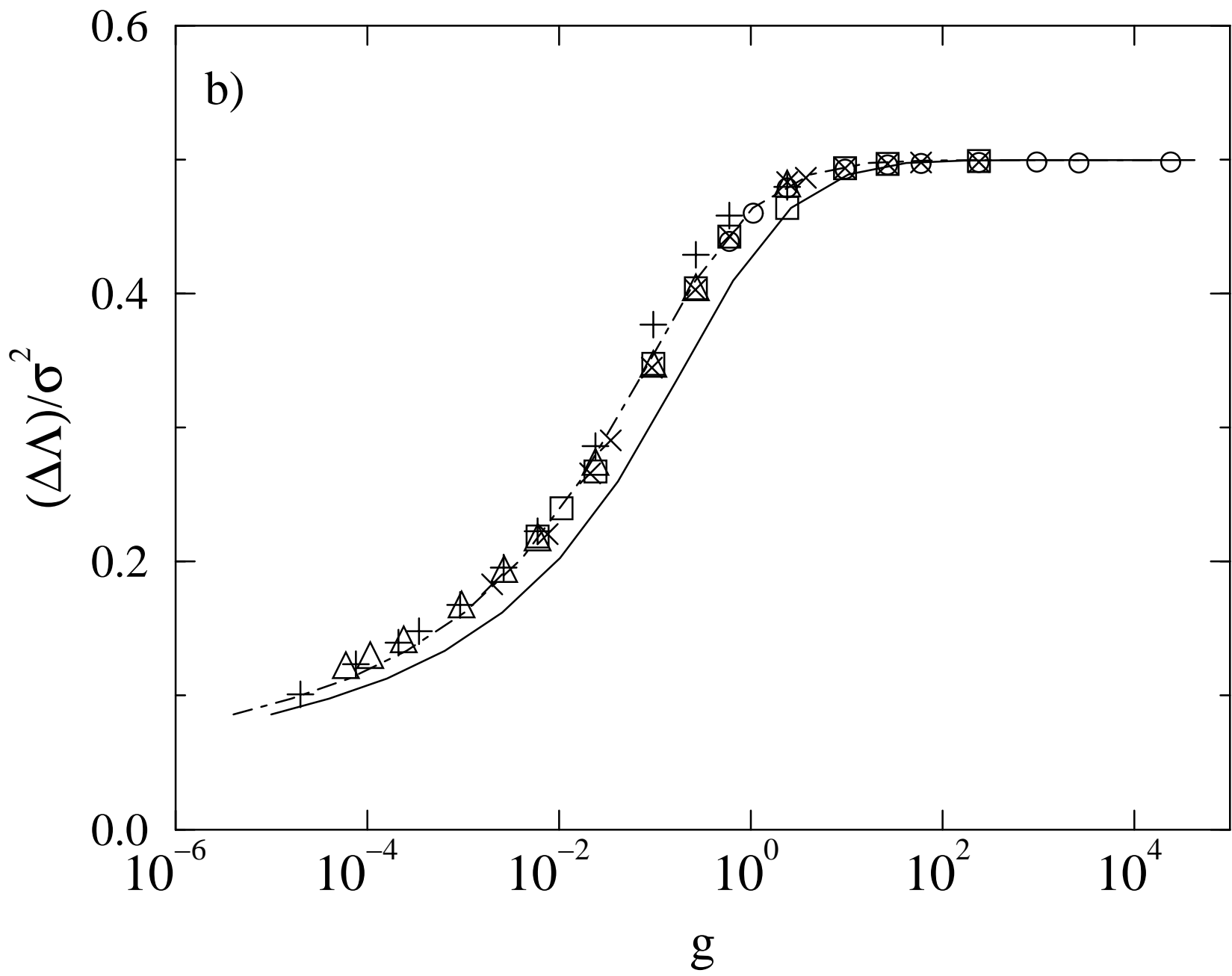
FIG. 3. Log-log plot of the probability distribution $P(R)$ to highlight the power-law behaviour. Circles, triangles and diamonds refer to $G = \sqrt{6} \cdot 10^{-2}$, $\sqrt{6} \cdot 10^{-3}$, $\sqrt{6} \cdot 10^{-5}$, respectively. The simulation details are as in Fig. 1. The various curves represent the analytical results as from Eq. (39).

FIG. 4. The Lyapunov exponent versus the scaling parameter G in the case of fluctuating multipliers. The Lyapunov correction $\delta\lambda$ is normalized so as to emphasize the $1/|\ln G|$ dependence. Circles correspond to $\varepsilon = 10^{-5}$ while diamonds to $\varepsilon = 10^{-3}$. The straight solid line represents the theoretical result (40).









Cecconi Politi Fig. 2b

Cecconi and Politi Fig.3

